

1

2

*Water Resources Research*

3

Supporting Information for

4

**Multi Attention Neural Network for Digital Rock CT Images Super-Resolution**

5

Zhihao Xing<sup>1</sup>, Jun Yao<sup>1</sup>, Lei Liu<sup>1</sup> and Hai Sun<sup>1</sup>

6

<sup>1</sup>Research Centre of Multiphase Flow in Porous Media, China University of Petroleum (East China), Huangdao District, Qingdao, China.

7

8

9

10 **Contents of this file**

11

12

Text S1

13

Figures S1 to S9

14

15 **Introduction**

16

- Experiments and algorithm details;

17

- Sample slices of training dataset;

18

- Data augmentation method in this research;

19

- The training log of the super-resolution models;

20

- Subplots of Figure 8 in the main article (Figures S4 to S6);

21

- Additional qualitative comparison on the coal test set and their difference maps;

22

- Additional qualitative comparison on the sandstone test set and their difference maps;

23

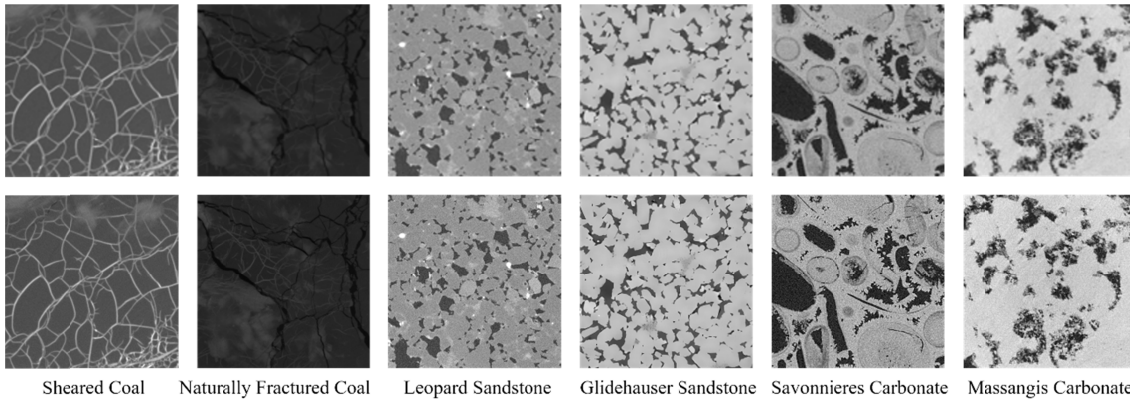
- Additional qualitative comparison on the carbonate test set and their difference maps.

24

26 **Text S1.**

28 Our codes are publicly available at [https://github.com/MHDXing/MASR-for-Digital-Rock-](https://github.com/MHDXing/MASR-for-Digital-Rock-Images)  
29 [Images](https://github.com/MHDXing/MASR-for-Digital-Rock-Images). All experiments and algorithm details are in this open source project.

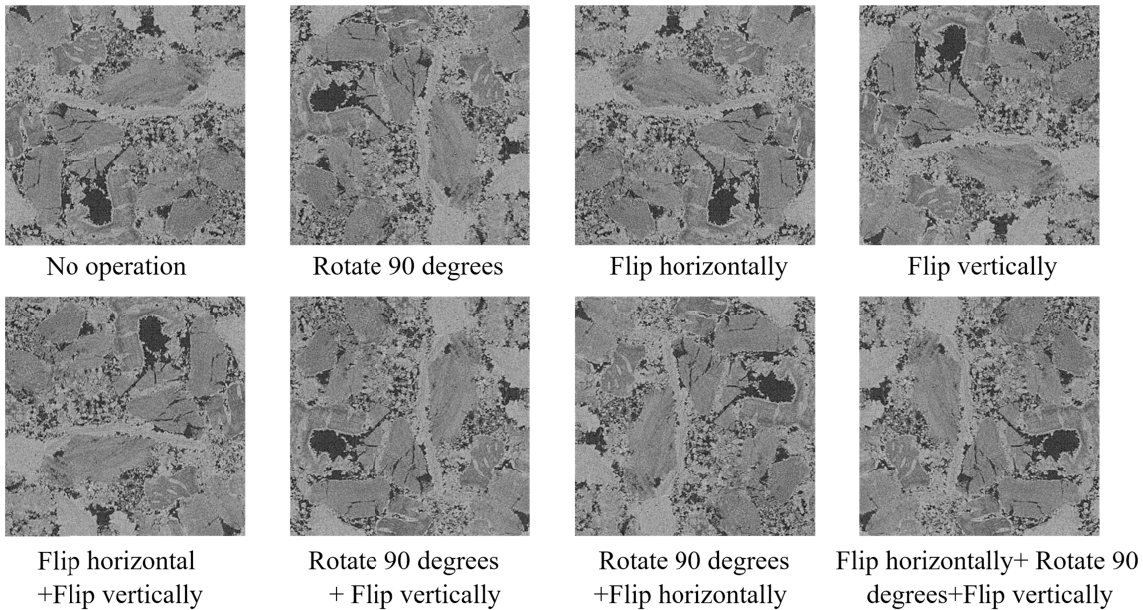
29



30

35 **Figure S1.** Sample slices of training dataset. First row: Low resolution images, i.e., inputs to the  
36 model. Second row: Corresponding high resolution images, i.e. ground truth. In the training  
37 stage, the model calculates the loss between the output and the ground truth, and optimizes  
38 the parameters by back propagation algorithm to make the output as close as possible to the  
39 ground truth

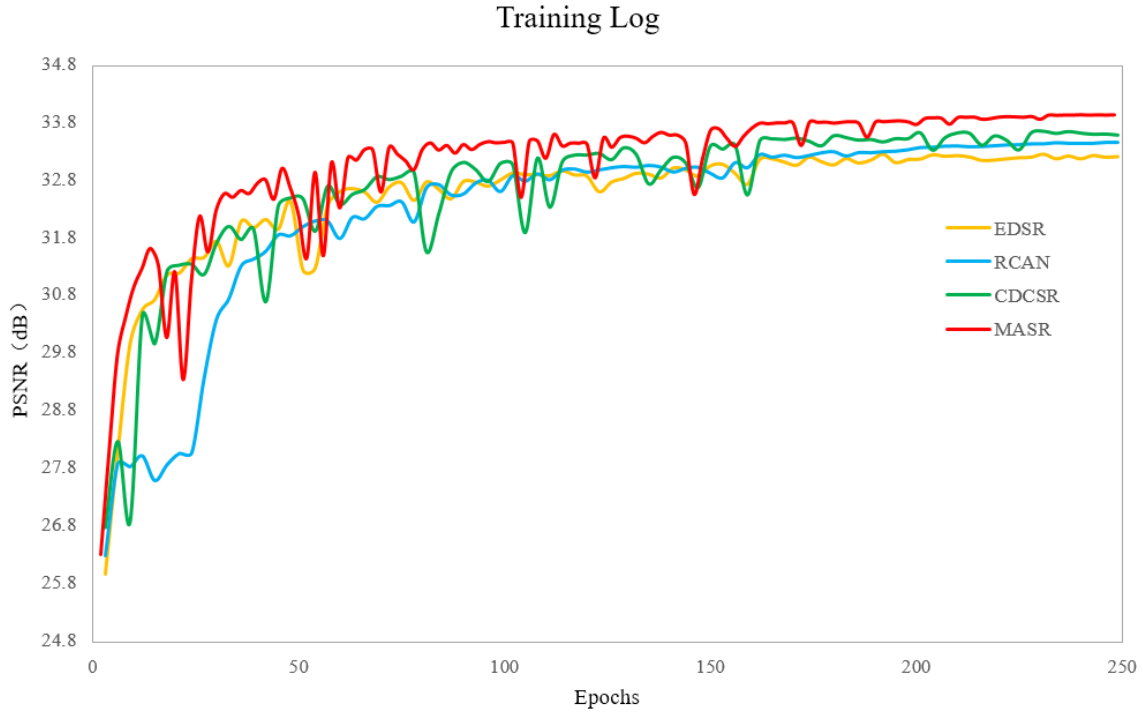
36



37

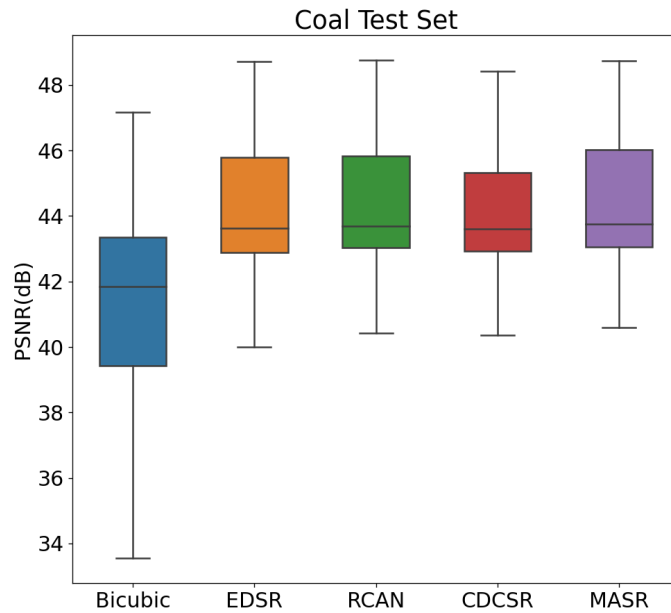
40 **Figure S2.** Data augmentation method in this research. In the training stage, the inputs are  
41 randomly flipped horizontally, flipped vertically or rotated to enhance the generalization of  
42 the model.

41



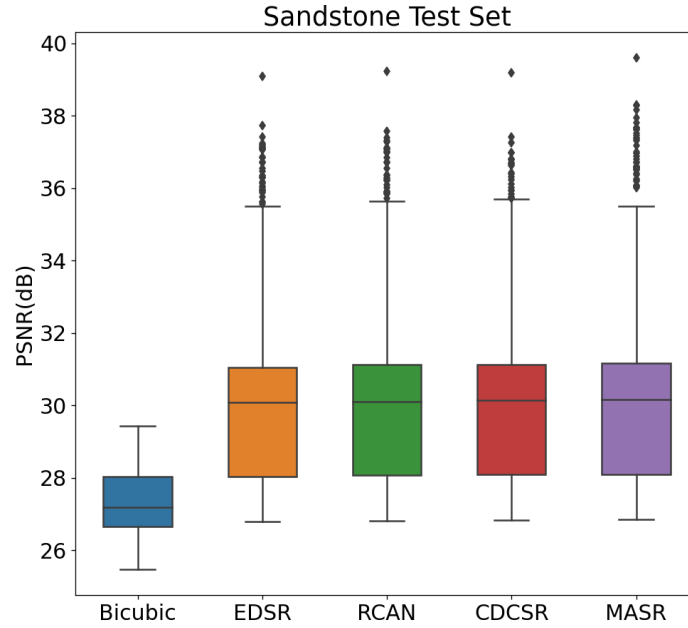
41

42 **Figure S3.** The average Peak Signal-to-Noise Ratio (PSNR) of the super-resolution models on  
 43 the validation set during training. Our proposed model (MASR) converges faster and better.  
 44



45

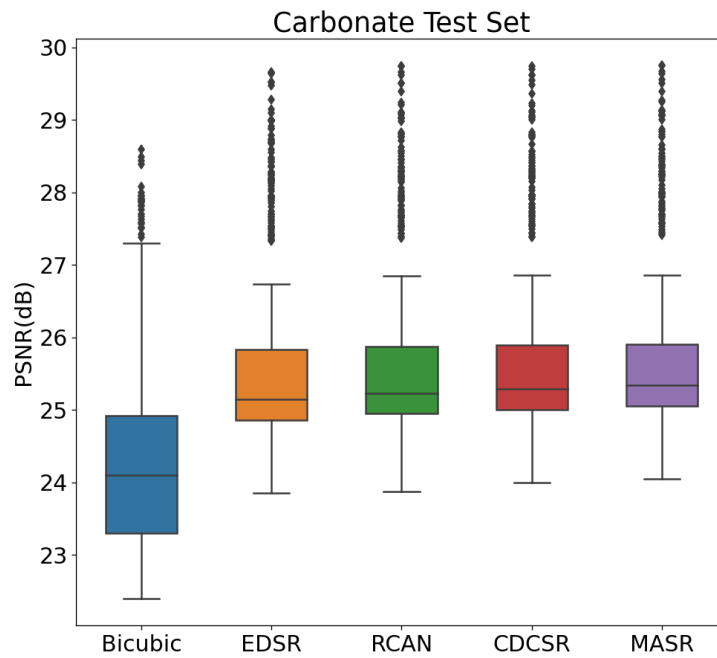
46 **Figure S4.** Boxplot of the average PSNR of EDSR, RCAN, CDCSR and MASR on coal test set. The  
 47 subplot of Figure 8 in the main article.



48

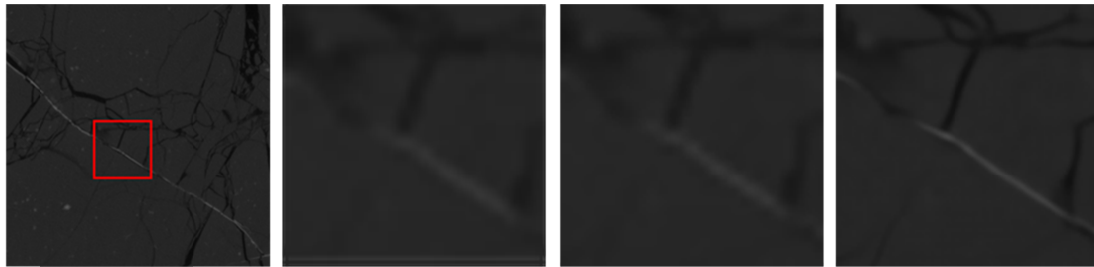
49 **Figure S5.** Boxplot of the average PSNR of EDSR, RCAN, CDCSR and MASR on sandstone test  
 50 set. The subplot of Figure 8 in the main article.

51



52

53 **Figure S6.** Boxplot of the average PSNR of EDSR, RCAN, CDCSR and MASR on carbonate test  
 54 set. The subplot of Figure 8 in the main article.

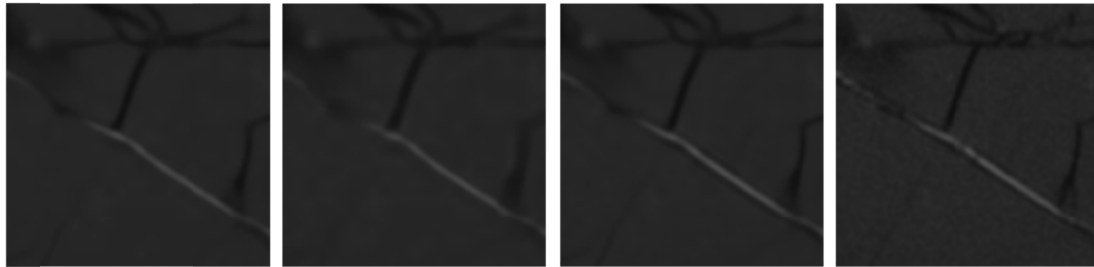


Coal

LR

Bicubic

EDSR



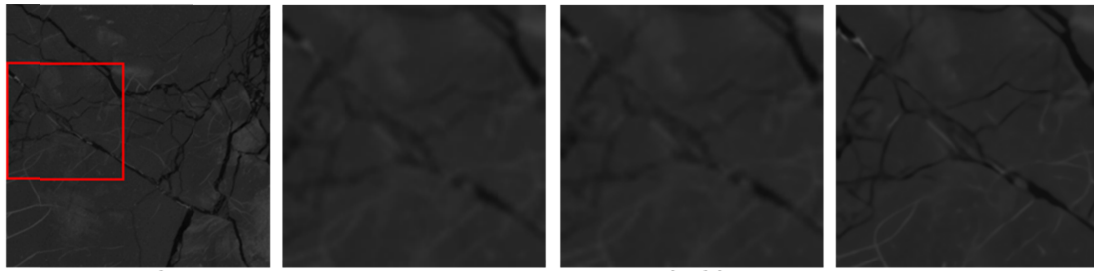
RCAN

CDCSR

MASR

HR

56

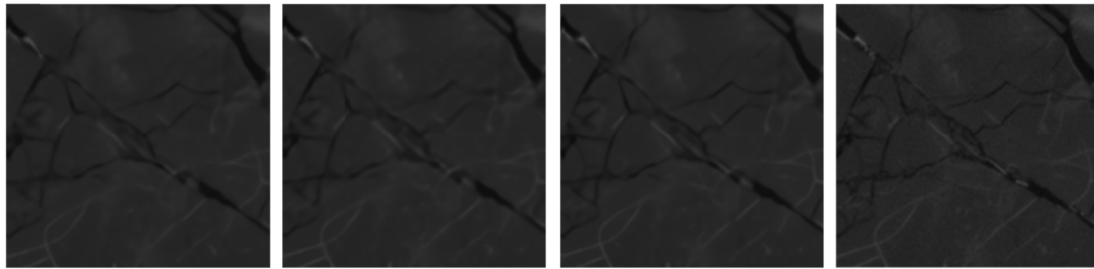


Coal

LR

Bicubic

EDSR



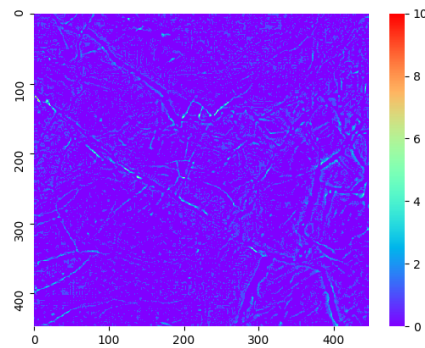
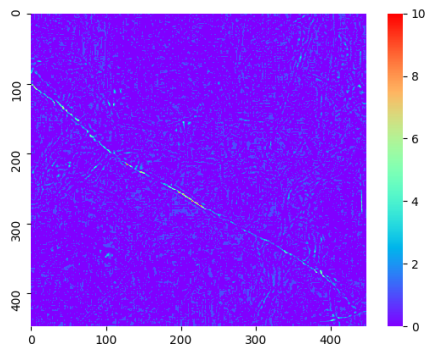
RCAN

CDCSR

MASR

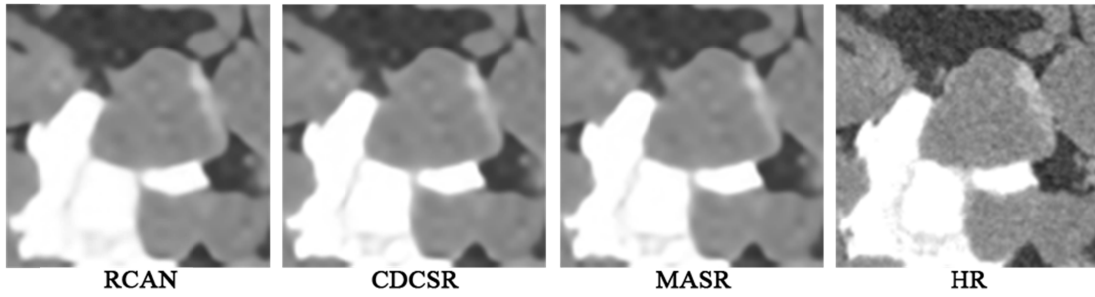
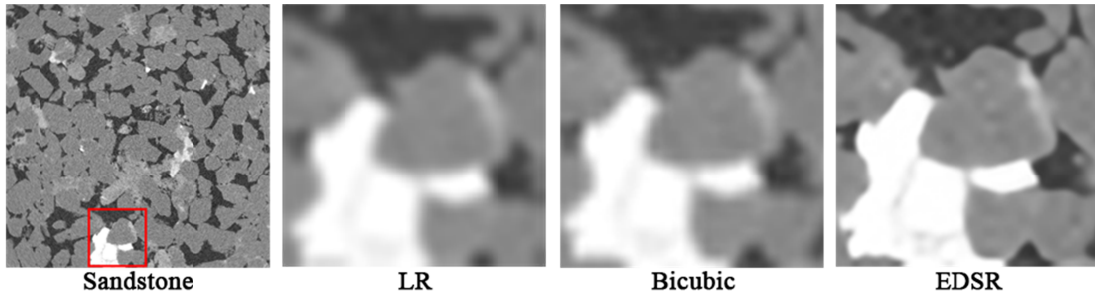
HR

57

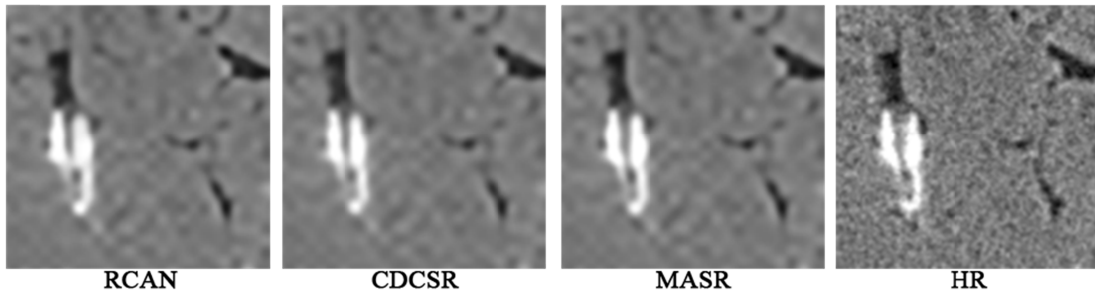
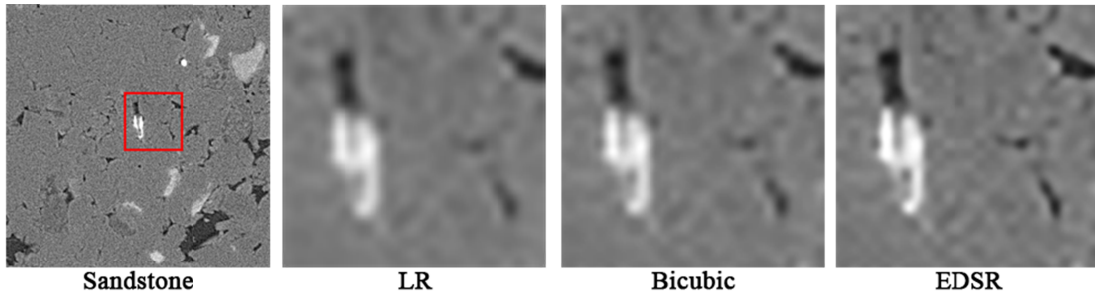


58

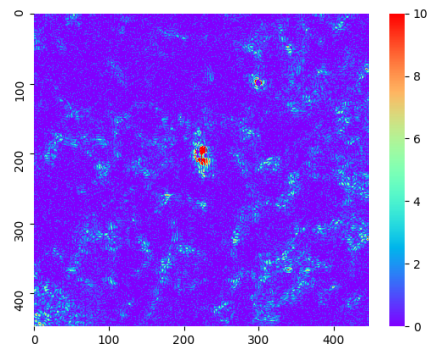
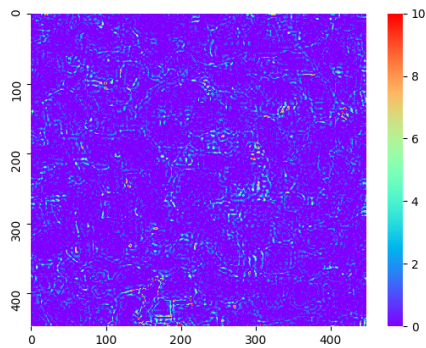
62 **Figure S7.** Additional qualitative comparison of our model with other works at  $\times 4$  SR on the  
 63 coal test set. Bottom: Difference maps of MASR and RCAN SR results in the above two sets of  
 64 images (MASR minus RCAN). The difference maps show that the edge recovered by MASR is  
 65 sharper.



63

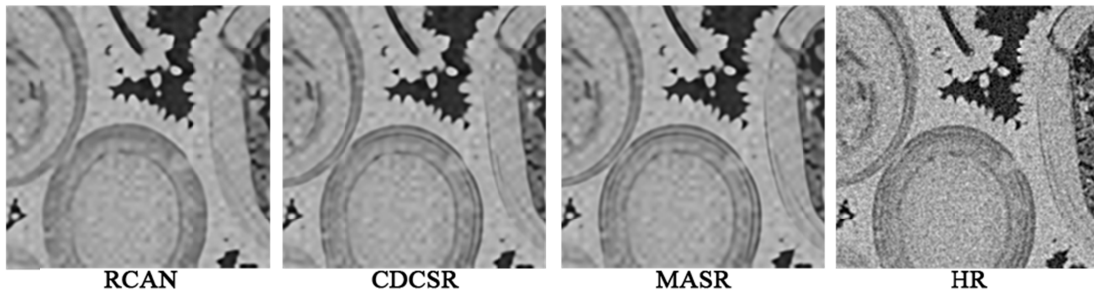
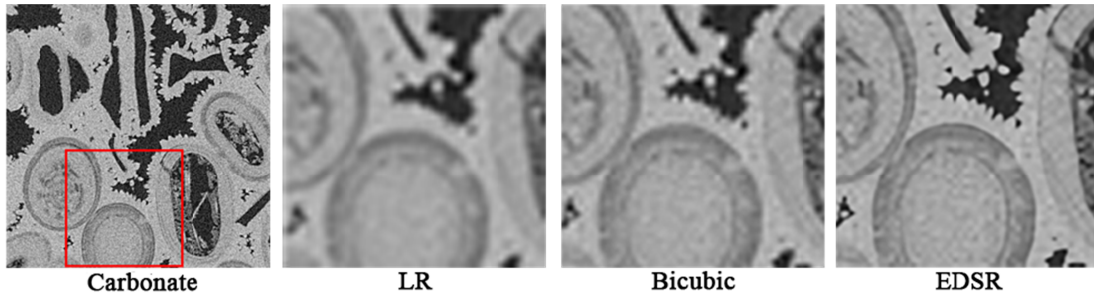


64

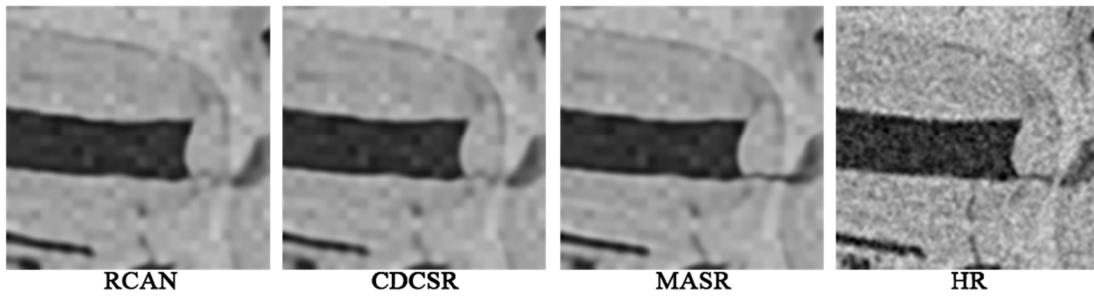
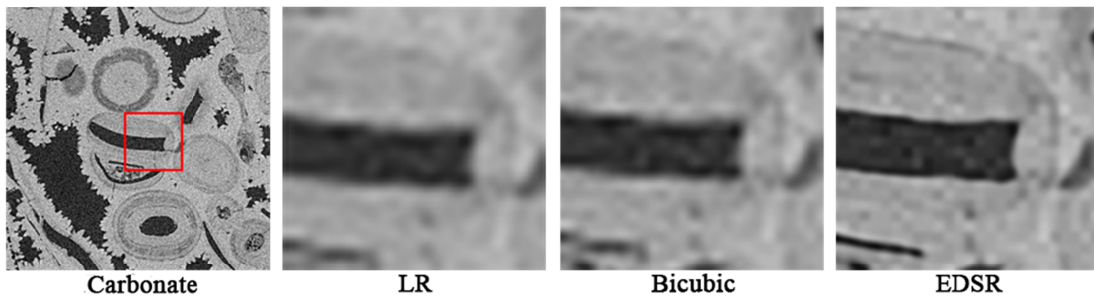


65

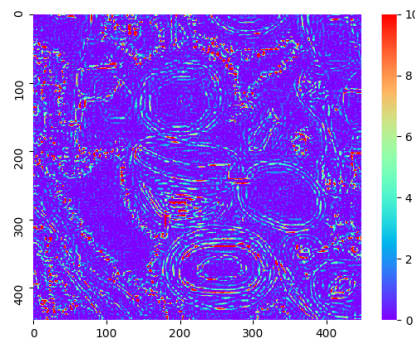
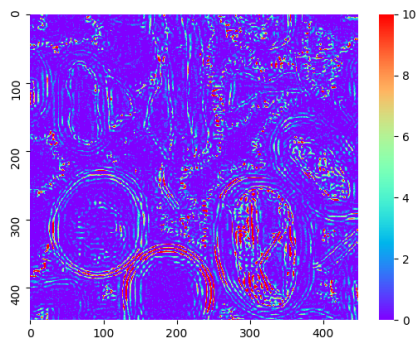
69 **Figure S8.** Additional qualitative comparison of our model with other works at  $\times 4$  SR on the  
 70 sandstone test set. Bottom: Difference maps of MASR and RCAN SR results in the above two  
 71 sets of images (MASR minus RCAN). The difference maps show that the edge recovered by  
 72 MASR is sharper.



71



72



72

76 **Figure S9.** T Additional qualitative comparison of our model with other works at  $\times 4$  SR on the  
 77 carbonate test set. Bottom: Difference maps of MASR and RCAN SR results in the above two  
 78 sets of images (MASR minus RCAN). The difference maps show that the edge recovered by  
 79 MASR is sharper.